Charles University

Faculty of Science

Study programme:

Applied geology

Mgr. Jakub Mareš

Vaporization plane and moisture-related characteristics of shallow subsurface zone of porous materials

Výparová fronta a vlhkostní charakteristiky přípovrchové zóny porézních materiálů

Doctoral thesis

Supervisor

doc. RNDr. Jiří Bruthans, Ph.D.

Consultants

Mgr. Martin Slavík, Ph.D.

Mgr. et Mgr. Tomáš Weiss, Ph.D.

Prague, 2024

Declaration of authorship

I hereby declare that this thesis was prepared and developed on my own. The work presented in this thesis has not been submitted for the application of any other professional degree. In the case of jointly authored publications, proper credit is explicitly indicated. All references and sources of information cited are listed at the end of this thesis.

In Prague

Jakub Mareš

Acknowledgements

I would like to thank my supervisor, Jiří Bruthans, who always supported me, helped to finance my research, and helped me to start my scientific career. I would also like to thank my consultants Martin Slavík and Tomáš Weiss, who helped me through all the pitfalls of my PhD studies and made it fun. I would also like to thank my colleagues, Michal Filippi, Nimrod Wieler, and Nurit Shtober-Zisu, who assisted me with the scientific papers.

This research was funded by Charles University Grant Agency (GAUK 265421), Czech Science Foundation (GAČR 19-14082S a 24-12696S), Technological Agency of the Czech Republic Gama (2021-2022): Development of a probe for the detection of liquid water in historical building materials. (TP01010040) Technological Agency of the Czech Republic Éta (2020-2023): Hidden beneath the surface. Archaeological terrains of Prague Castle, their protection and presentation in the modern world. (TL03000603). This research was also supported by the UNCE/SCI/006 Center for Geosphere Dynamics and Johannes Amos Comenius Programme (P JAC), project No.CZ.02.01.01/00/22_008/0004605, Natural and anthropogenic georisks.

Contents

Abstract

Moisture in porous rocks causes material degradation and weathering. However, very little is still known about its dynamics, spatial distribution, and sources. This thesis presents three examples of the study of moisture distribution and fluxes in rock outcrops with cavernous weathering forms: coastal honeycombs in Italy, tafoni in a humid climate near Kralupy nad Vltavou, Czechia and the transition from inland notches to tafoni in carbonates in Israel. At all sites with tafoni and honeycombs, the depth of the evaporation front inside the caverns is closer to the surface than outside most of the time, except after heavy rainfall or, in the case of the coastal area, after more intense surf. The lower depth leads to a higher evaporation rate from the caverns and higher precipitation of salts, causing active salt weathering there. For the first time, the spatial and temporal distribution of the evaporation front on outcrops with cavernous weathering has been determined. This allows a better understanding of the evolution of these forms. For the first time, the amounts of precipitated salts were calculated from evaporation rates for natural rock outcrops. At the Kralupy site, water influxes and outfluxes from/to the tafoni were determined, from which a water balance of the arcosic sandstone outcrop was constructed. The results presented here show that knowledge of the moisture distribution and the determination of the evaporation rate are essential for understanding and quantifying weathering processes and for determining the water balance of rock outcrops.

Abstrakt

Vlhkost v porézních horninách způsobuje degradaci materiálu a jeho zvětrávání. Přesto je stále velmi málo známo o její dynamice, prostorovém uspořádání a jejích zdrojích. Tato práce prezentuje tři příklady studia vlhkosti na skalních výchozech s výskytem kavernózního zvětrávání: přímořské voštiny v Itálii, tafoni v humidním klimatu u Kralup nad Vltavou v Česku a přechod z inland notches do tafoni v karbonátech v Izraeli. Na všech lokalitách s tafoni a voštinami je většinu času hloubka výparové fronty uvnitř kaveren blíže k povrchu než vně, opačně je tomu pouze po vydatnějších deštích nebo v případě přímořské oblasti po intenzivnějším příboji. Poprvé bylo stanoveno prostorové a časové rozložení vlhkosti na výchozech s výskytem kavernózního zvětrávání, což umožňuje lépe pochopit problematiku vzniku těchto forem. Poprvé byly pro přírodní výchozy spočítány intensity výparu a množství vysrážených solí. Na lokalitě Kralupy byly stanoveny množství vody vystupující/vstupující z/do tafoni, z čehož byla následně sestavena vodní balance pískovcového výchozu. Prezentované výsledky ukazují, že znalost rozložení vlhkosti a stanovení intenzity výparu je zásadní pro pochopení a kvantifikaci zvětrávacích procesů a umožňuje stanovit vodní bilanci skalních výchozů.

Introduction

This doctoral thesis is comprised of three peer-reviewed publications that have been published in impact factor journals. These publications address the topic of moisture in the unsaturated zone near the surface of porous rocks.

The spatial and temporal distribution of moisture content has a profound impact on material strength, frost, and salt weathering (Huinink et al., 2004; Matsuoka and Murton, 2008; Bruthans et al., 2018), karstification (Shtober-Zisu et al., 2015; 2017) and biological activity (Slavík et al., 2017). Water may be present in any porous material. Water serves as a transport medium for salts, which concentrate and precipitate at the evaporation front, where they cause the greatest destruction of material by salt weathering (Huinink et al., 2004; Bruthans et al., 2018; Safonov and Minchenkov, 2023). Water originates from a variety of sources, including infiltration of precipitation water, inflow from rock interior, or condensation of atmospheric moisture (McBride and Picard, 2000; Goudie et al., 2002; Brandmeier et al., 2011). Water can exist in porous materials in all phases, including solid, liquid, and gas. In its solid form (ice), water is immobile. In its liquid form, it flows against the direction of the hydraulic gradient, based on the Darcy-Buckingham equation (Buckingham, 1907). In its gaseous form, it flows based on Fick's law (Fick, 1855).

The moisture content of porous materials can be determined by a variety of methods that employ different physical properties. These methods can be divided into two categories: destructive and non-destructive. The gravimetric method represents the most accurate approach for determining moisture content. This method involves the collection of an undisturbed sample and subsequent weighing of the sample in its natural and dried state (Smugge et al., 1980).

However, the high degree of destructiveness precludes repeated use on rock outcrops. The most well-known non-destructive methods are electrical methods, such as the protimeter (which measures the electrical conductivity between electrodes with constant distance) or electrical resistivity tomography, which measures the resistivity of the environment and takes advantage of the fact that wet environments conduct electricity better than dry materials (Schnepfleitner et al., 2016). A significant limitation of electrical methods is the influence of salinity, which affects the electrical resistivity of the material. This makes measurements by electrical methods in the near-surface zone of natural outcrops highly uncertain (Weiss and Sass, 2022). Conversely, electromagnetic methods (most commonly TDR – time domain reflectometry) assess the dielectric permittivity of the environment. This value is 80 for water, but 1-5 for air and rock minerals. Consequently, even minor quantities of water permit the precise measurement of moisture content (Smugge et al., 1980). Moreover, this method is far less susceptible to salinity than electrical methods. Furthermore, moisture content can be calculated from the measured suction pressure, provided that the retention curve for a given material is known. The advantage of this method is the point information of the moisture content. However, there are also disadvantages, including the risk of error in determining the retention curve and the impossibility of measuring at high suction pressures. Other methods, such as thermal pulse, infrared tomography, and neutron methods, are unsuitable for regular moisture measurements in the near-surface zone of porous materials in nature due to their complexity and/or large error and can only be used in the laboratory (Churayev and Rode, 1966; Weiss and Sass, 2022; Weiss et al., 2022).

To better interpret moisture measurements and understand moisture dynamics in the near-surface zone of rocks, it is essential to understand the depth of the evaporation front. The evaporation front is the boundary in the porous material that separates the capillary zone from the dry surface layer (Idso et al., 1974; Hillel, 2004; Or et al., 2013). While water in the capillary

zone is primarily in the liquid state, in the dry surface layer it is present only as water vapor. This was verified by laboratory experiments. Despite its importance, the evaporation front was only determined indirectly by moisture measurement methods until 2020 in porous rock in the field. In 2020, a new microdestructive method was developed that directly measures the depth of the evaporation front below the surface in porous rock (Weiss et al., 2020). This method employs sodium fluorescein dye, which is glued to a surgical needle (Fig. 1). The prepared probe is then inserted into a pre-drilled hole, where it reacts with the porous rock. The fluorescein begins to dissolve on the probe's surface in the capillary zone, resulting in a color change from dark red to green. In contrast, the probe remains unaltered in the dry surface layer. The depth of the evaporation front is determined by measuring the length of the probe that is in the dry surface layer (from the rock surface), with the red color unchanged. This method can accurately detect the evaporation front. Evaporation front depth is one of the critical parameters to calculate the evaporation rate because the depth of the evaporation front determines the vapor diffusion path, which is the parameter for determining the intensity of vapor transport according to Fick's law.

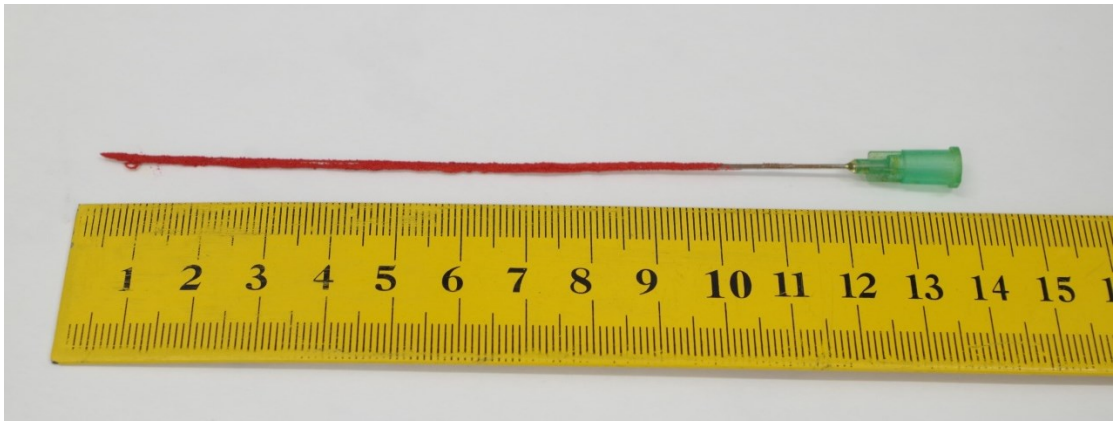

Figure 1: Prepared uranine-probe before measurement.

In order to determine the water balance of rock outcrops, it is of the utmost importance to determine the evaporation rate. Evaporation progress in time can be divided into three phases when considering constant evaporation demand (Idso et al., 1974; Hillel, 2004; Or et al., 2013). In the initial phase, the evaporation front is situated on the surface of the studied material. During this phase, the evaporation rate is the highest, approaching the potential evaporation rate, and relatively constant over time.

In the second phase, the evaporation front is receding. During this phase, the evaporation rate decreases as water passes through the increasing thickness of the dry surface layer in the form of water vapor (Lehmann et al., 2008; Or et al., 2013).

In the third phase, the evaporation front is deep, and residual moisture is evaporated. During this phase, the evaporation rate is minimal and remains constant over time.

To estimate the evaporation rate in the catchment scale, empirical equations are typically employed to calculate evapotranspiration based on meteorological data, including temperature, relative humidity, solar radiation, and wind speed. The most commonly utilized equation is the Penman-Monteith equation (Allan et al., 1998). These equations are convenient for calculations in catchment scale; however, they have two significant disadvantages. First, they are data-intensive, which makes them impractical for use in many situations. Second, they do not provide accurate point values. More accurate methods for measuring evaporation from the soil environment include the use of lysimeters, atmometers, or evaporation cups (Manning, 2016; Gavilán and Castillo-Llanque, 2009). However, these methods are not applicable for measurements in rocks, as they do not allow for placement in hardened material.

In rocks, the evaporation rate can be calculated from the depth of the evaporation front, as this has a direct influence on the evaporation. The closer the evaporation front is to the surface (the

smaller the depth), the greater the evaporation rate. This relationship is given by Fick's first law (Fick, 1855):

$$e = \delta \frac{\Delta P}{L} \quad (1)$$

where e is the evaporation rate (kg/m^2/s), δ is the diffusion coefficient (s), ΔP is the difference in partial pressures at the evaporation front and at the surface of the studied material (Pa), and L is the depth of the evaporation front (m).

The higher the evaporation rate, the more salts are precipitated and the greater the weathering of the material. The evaporation rate is also affected by the presence of deliquescent salts. Deliquescent salts absorb moisture from the air and dissolve in it when the relative humidity increases above the deliquescence relative humidity of a given salt.

Typical examples of salt weathering include the formation of honeycombs and tafoni (Fig. 2). Tafoni are meter-long caverns bounded by vizors that protect them from precipitation (McBride and Picard, 2000; André and Hall, 2005). Honeycombs are smaller forms, generally less than ten centimeters in size. They typically occur in clusters, with individual caverns separated from each other by lips (Sunamura, 1996). Inland notches are horizontal caverns with vertical C-shaped cross-section developed in carbonate rocks extending in a horizontal direction over tens of meters. Inland notches are related to subaerial karstification of carbonate layers exhibiting slight variation in porosity which allows for faster erosional retreat of a more porous layer (Shtober-Zisu et al., 2015, 2017, 2020). Cavernous weathering is most prevalent in arid and semi-arid regions, as well as coastal areas. However, it has been documented in all climatic zones across the Earth (Mustoe, 1982).

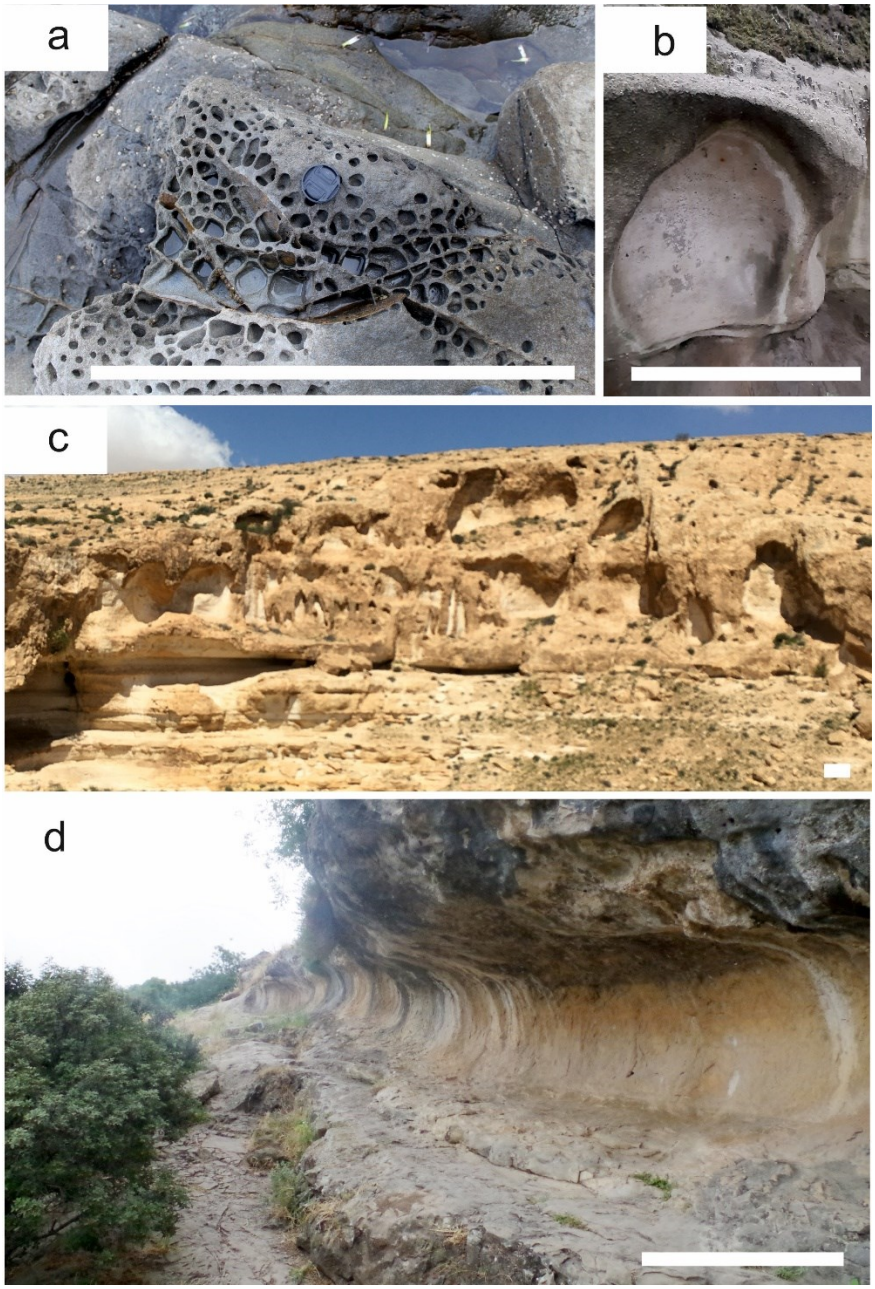

Figure 2: Typical cavernous weathering forms: a) honeycombs in Italy, b) tafone in Czechia, c) tafoni in Israel, and d) inland notch in Israel. Scale bars equal 1 m.

Although the majority of authors concur that cavernous forms are the result of salt weathering (Mottershead, 1994; Rodrigues-Navarro et al., 1999), there is still no consensus on the mechanism by which caverns deepen on one side when the surface next to it remains stable. Some authors posit that the formation of cavernous forms is due to the hardening of the rock surface, which results in the formation of a resistant layer (case hardening; Conca and Rossman,

1982; Viles and Goudie, 2004). Conversely, others attribute the formation to the action of wind, which causes the surface to dry out (Rodriguez-Navarro et al., 1999). The most recent hypothesis is the hydraulic hypothesis, which states that water preferentially flows into cavities where the evaporation front is closer to the surface. In these cavities, salt precipitation is more intense, thus deepening the cavities occurs (Huinink et al., 2004).

There have been many studies that have focused on the description of cavernous weathering forms, but none that have gone into detail on the determination and quantification of moisture, determination of water fluxes, and quantification of precipitated salts, and have compared moisture behavior in different forms from different locations with each other.

Aims of the thesis

Previously published procedures to determine the depth of the evaporation front (Weiss et al., 2018; 2020) and the ability to determine the evaporation rate (Slavík et al., 2020; 2023) recently allowed for the quantification of salt deposition in different parts of the landform and the quantitative verification of the processes involved in water and dissolved salts transport and precipitation. The combination of evaporation front measurement, calculation of evaporation rate, and measurement of mechanical properties of studied rocks potentially allows to determine the processes responsible for the formation of cavernous weathering forms. The focus of this work is to combine these techniques to better describe moisture distribution and fluxes in rock subsurface.

On the Italian Mediterranean coast, well-developed honeycombs occur in metasandstone. There are many hypotheses on the origin of coastal honeycombs. The aim of this paper was to describe the moisture and strength characteristics and to calculate the evaporation rate and the amount of precipitated salts separately for the pits and walls of the honeycombs. For this purpose, the depth of the evaporation front, the tensile strength, and the chemical composition of the salts were measured. The fundamental characteristics of the studied material were established in a laboratory, and an evaporation experiment was conducted on an experimental block.

In Israel, a pronounced climatic gradient is observed over a distance of only hundreds of kilometers, from a Mediterranean climate with an annual rainfall of 600 mm to hyperarid areas with an annual rainfall of 20 mm only. The same carbonate layer is present throughout the climatic zones. A variety of cavernous weathering phenomena, including tafoni and inland notches, are observed in these regions. This provides an optimal setting for investigating the impact of climate on the formation of cavernous weathering forms. To this end, spatial distributions of moisture and tensile strength were quantified for these forms. The aim of this

paper was to compare the hydraulic and mechanical characteristics of different weathering forms and to describe the effect of climate on cavernous weathering forms.

The area of Kralupy nad Vltavou is notable for the presence of outcrops of arkosic sandstone with perfectly developed tafoni. The accessibility of these forms allows for regular moisture measurements, which permit the determination and quantification of water fluxes in porous rock. This provides unique data on the temporal and spatial distribution of water in the tafoni, which may advances the understanding of the origin and evolution of these forms. The objective of this paper was to determine the spatial and temporal distribution of moisture and, based on this, the water fluxes and water balance of the outcrop.

Contributions of individual authors to joint papers

In the paper *Coastal honeycombs (Tuscany, Italy): Moisture distribution, evaporation rate, tensile strength, and origin* I conducted the majority of the measurements in the field and in the laboratory, including the evaporation experiment. Then, I evaluated the data and wrote a paper based on the results. I consulted with Jiri Bruthans on all the steps of the process, and he also performed some of the measurements and edited the text of the paper. Tomas Weiss provided assistance with the preparation of the paper, while Michal Filippi conducted a portion of the laboratory measurements and undertook the editorial revision of the final text.

In the paper *Climate controls on limestone cavernous weathering patterns,* I was responsible for designing and conducting the majority of the field and laboratory measurements, evaluating the resulting data, and writing the article. Tomas Weiss provided assistance with field measurements and the preparation of the paper. Nimrod Wieler and Nurit Shtober-Zisu provided editorial assistance in the preparation of the final text.

In the paper *Moisture patterns and fluxes in evolving tafoni developed in arkosic sandstone in temperate climate,* I designed and performed the majority of the measurements in both the field and laboratory settings. I then proceeded to evaluate the measured data and subsequently wrote the paper based on these results. Jiří Bruthans served as a supervisor in the preparation of the measurements and writing of the paper. Alžběta Studencová conducted a portion of the measurements, while Michal Filippi provided assistance with the text.

Methods

Field measurements

The tensile strength

One of the consequences of weathering and subsequent disintegration of the material is a reduction in its tensile strength (Gregory and Goudie, 2011). Tensile strength measurements allow for the identification of weakened areas with an increased risk of rock decay (Bruthans et al., 2014). In general, there are several ways to measure rock strength, some of which are established and generally accepted methods. The use of unconfined compressive strength and Brazilian tensile strength at samples taken is not recommended due to their destructive nature. Less destructive methods that are often used for field measurements of rock strength are proxy methods for measuring hardness, such as the Equotip or Schmidt hammer (Viles et al., 2011). However, the impact of such instruments is too destructive that it makes it impossible to measure the most intensely weathered material. Therefore, a novel method is employed in which a 2×2 cm aluminum T-profile is affixed with epoxy glue to the studied surface (Fig. 3; Bruthans et al., 2012). Once the adhesive has hardened, a force gauge is used to apply a gradually increasing tensile force perpendicular to the surface until the material fails. The tensile strength (Pa) is then calculated as the maximum force at the time of tearing (N) divided by the area torn off (m^2). This method allows the measurement of even heavily weathered and uneven surfaces.

Figure 3: Measurement of tensile strength using pull-off test (Mareš et al., 2024a).

Drilling resistance

Drilling resistance was measured using a drilling machine PZZ 01 (Technický a zkušební ústav stavební Praha) with a 5 mm diameter drill bit (Fig. 4). The drilling machine was subjected to a defined force compressing the drill bit and operated for a controlled number of rotations in percussion mode. Thereafter, the depth of the hole was gauged with the caliper. A higher drill depth thus indicates a softer material. The resulting values were adjusted for the wear of the drill bit (its sharpness decreases with drilling) by adding a correction factor calculated from the difference in depths of drilled holes in a homogeneous practice sample before and after the presented measurements.

Figure 4: Drilling machine for testing drilling resistance.

The depth of the evaporation front

The depth of the evaporation front was measured using the uranine-probe method (Fig. 1; Weiss et al., 2020): A 32-cm stainless steel probe coated with Na-fluorescein was inserted into a pre-drilled 2-10 mm wide hole that had been air-flushed. After ten minutes, the uranine-probe was taken out and interpreted: the presence of capillary water caused the Na-fluorescein dye to dissolve and change its color from red to green.

Suction pressure

Suction pressure, together with elevation, controls the flow direction of capillary water. In Czechia, suction pressure was measured using microtensiometers T5x with an INFIELD7 reader (UMS, Germany). Holes were drilled into the tafone at depths ranging from 0.5 to 10 cm. Shallow holes were 0.5 to 2 cm deep, and deeper holes were 10 cm deep.

Moisture content

Volumetric rock moisture measurements from the surface to a depth of 90 cm were made using a precise SONO-ES T3 (TDR; IMKO, Germany) in the tafone in Czechia on both the outer surface and inside the cavern in 22 mm diameter holes stabilized with plastic tubes. The measured values were converted to volumetric moisture content by calibration on an arcosic sandstone block in the laboratory.

The infiltration rate

The infiltration rate was measured using Karsten tubes using a modified method according to Hendrickx (2013): Glass tubes with enlarged mouths with a contact area of 5.7 cm^2 were attached to both horizontal and vertical surfaces using a Bantex poster adhesive with a consistency of plasticine (Fig. 5). The amount of water infiltrated from the tube to the rock over time was recorded. The measurement time ranged from seconds to days, depending on the infiltration rate.

Figure 5: Measurement of the infiltration rate using Karsten tube (Mareš et al., 2024a).

The salt composition of the rock

To determine the composition and concentration of salts in the rock, the drilled material was collected from various depths (0-1, 1-2, 2-4, and 4-8 cm) following the procedure of Karatas et al. (2022): A hand drill in percussion mode equipped with a 1 cm diameter drill bit was used to collect drill dust samples. To minimize cross-contamination between sampling depths, the drill bit was meticulously cleaned with a thin cellulose tissue after each sample collection. Additionally, the borehole was purged with compressed air to remove any residual dust particles.

The effect of air humidity condensation on the ambient water source was monitored using two cores covered by epoxy on all but one side, placed into the tafone, sheltered from the rain, and periodically weighed. To characterize the study site in terms of its climate and to calculate evaporation from the rock, long-term monitoring of the air temperature and relative humidity

was performed. Data was recorded every 30 minutes using Voltcraft DL-121TH temperature and relative humidity dataloggers embedded in the rock with the logger on the surface.

Laboratory measurements

The salt composition from sampled dust was analyzed in the laboratory. The samples were dried, crushed, weighed, and leached in deionized water (1 g of crushed rock per 100 ml of water), shaken at 150 rpm for 12 h, and the leachates were filtered with a 0.45 μm filter. The solution was analyzed by inductively coupled plasma atomic emission spectroscopy (ICP-OES, Thermo Scientific, Waltham, MA, USA) for cations (Ca, Na, Mg, K) and by high-performance liquid chromatography (HPLC, Dionex ICS-2000, Thermo Scientific, Waltham, MA, USA) for anions (HCO_3, SO_4, Cl, NO_3).

To characterize the evaporation dynamics under controlled conditions, a block of the Italy metasandstone, partly covered by honeycombs was immersed in 0.55 mol/L NaCl solution to simulate wetting of the rock during storms by sea water. After saturation, the block was left to dry (Fig. 6) under infrared heating for 12 h/d, simulating the Mediterranean summer climate. The block was placed in a plastic dish with a salt solution and a piece of cotton cloth, which simulated a source of water from the massif and prevented evaporation from the other sides except for the surface with the honeycombs. The cotton cloth ensured capillary contact between the reservoir and the block. During drying, relative humidity and temperature of the air surrounding the block were measured, the block was repeatedly weighted, and the evaporation front depth and relative surface moisture were measured at 12 points (six in the pits and six in the lips).

Figure 6: A testing of evaporation dynamics on a metasandstone block with honeycombs. The block is placed in a plastic dish with a piece of cotton cloth, which serves as a capillary water inflow path to the block. Narrow drill holes to measure the depth of the evaporation front are highlighted by an orange zone of uranine dye (Mareš et al., 2022).

Pore size distribution characterizes the resistance to salt and frost weathering (Mal'a and Greif, 2021). The pore size distribution and porosity were determined using the high-pressure mercury porosimetry technique. The samples (3 g of rock pieces up to 0.5 cm^2 in size) were dried at 105 °C for 24 h in a vacuum (1 Pa) prior to analysis. They were then placed in the AutoPore IV 9520 instrument (Micromeritics, Norcross, GA, USA) for determination of intrusion volume, bulk density and pore size distribution. Recalculation of pressures to pore radii was performed using the Washburn (1921) equation. The AccuPyc II 1340 pycnometer (Micromeritics) was used to determine the skeletal (true) density using 99.9995% pure helium. The pore size distribution was measured at the Institute of Geology of the Czech Academy of Sciences.

Retention curve measurements were performed using a modified method described by Angerer and Birle (2016). Moisture content was measured gravimetrically with an accuracy of 0.1 g and a standard deviation of 0.05 g. Suction pressure was measured using T5x microtensiometers (UMS, Germany). The measurement was carried out on core samples with a diameter of 75 mm

and a length of 60 mm. In each core, two 20 mm deep, 5 mm diameter holes were drilled for suction pressure measurements. The samples were saturated with water in a vacuum and then the suction pressure was measured in both holes. The resulting value of suction pressure for a given moisture content was the average of these two measurements. After measurement, the samples were allowed to evaporate to the next measured weight. When the weight was reached, the samples were sealed between two plastic lids, taped and left to homogenize for 1 to 3 days. After homogenization, the samples were reweighed, and the suction pressure measured. A total of 16–20 measurements were performed. The measurement was stopped when the suction pressure exceeded 180 kPa, as hydraulic contact of the tensiometer with the core was no longer possible. The samples were dried then in an oven at 105°C and their dry weight was measured. The moisture content from the retention curve (θ) was calculated using the equation of Van Genuchten (1980):

$$\theta = \theta_r + \frac{(\theta_s - \theta_r)}{(1+|\propto h|^n)^m} \quad (2)$$

where θ_s is the saturated moisture content, θ_r is the residual moisture content, h is the pressure head (m), α, n and m are fitting parameters.

Vapor diffusivity is an important parameter for characterizing the permeability of a porous material to water vapor. The vapor diffusivity coefficient was determined for cores according to EN ISO 12572:2001 using the wet cup method (Pavlík et al., 2008; Slavík et al., 2017). A core with a diameter of 75 mm and a length of 50 mm was placed in a polyvinyl chloride (PVC) cup and sealed with epoxy resin on the cylindrical sides so that all vapor flow was through the core only. Another PVC cup, which acted as a source of 100% humidity, was partially filled with distilled water and attached to the cup with the core using electrical tape. Only water vapor was allowed to diffuse upwards due to the empty space between the water and the core (Slavík et al., 2020). This setup was placed in a CTC 256 climatic test chamber (Memmert, Schwabach,

Germany) with a pre-set relative humidity of 50% and a temperature of 20°C. This created an air humidity gradient that caused water vapor to diffuse through the core. The amount of evaporated water was measured by repeatedly weighing the setup over 28 days. The water vapor diffusion coefficient was measured at the Institute of Rock Structure and Mechanics of the Czech Academy of Sciences.

The saturated hydraulic conductivity was measured using a Darcy's Law apparatus (Tan, 1989). The Darcy's Law apparatus allows water to flow through a cylindrical core, the sides of which are sealed with epoxy resin in a PVC tube. The samples were saturated with water in a vacuum and placed on the Darcy's Law apparatus. The saturated hydraulic conductivity K (m/s) was calculated using the equation (Tan, 1989):

$$K = -\frac{sl}{S\Delta t} ln \frac{h_0}{h_1} \quad (3)$$

where s is the cross-sectional area of the tube [m^2], l is the length of the core [m], S is the cross-sectional area of the core [m^2], Δt is the measured time step [s], $h0$ is the height of water in the tube at the beginning of the measurement [m], and h_1 is the height of water in the tube at the end of the measurement [m]. All measured parameters are summarized in Table 1.

Calculations

The evaporation rate was calculated according to Slavík et al. (2020), using Fick's equation (eq. 1). If the evaporation front is situated at the surface or close below the surface, the parameter β is employed instead of L to represent the thickness of the saturated air layer above the surface of the material (Slavík et al., 2023). The partial pressure of water vapor can be calculated using the Tetens (1930) equation:

$$P = 0.61078 exp \frac{17.27T}{T+237.3} \times 1000 \quad (4)$$

where T is the temperature (°C). In the case of an unsaturated water vapor environment, the resulting value must be multiplied by the degree of air humidity saturation (RH/100). The influx to the outcrop was calculated from the water balance as:

$$I = E + \Delta S \quad (5)$$

where I is the water influx, E is the evaporation rate and ΔS is the change in storage at the evaporation front.

The quantity of precipitated salts, designated as M (g/m^2/year), can be calculated using the following equation:

$$M = e_r \times c \quad (6)$$

where e_r represents the annual evaporation rate from the rock surface (kg/m^2/year) and c denotes the concentration of salts in the capillary water (kg/m^3).

For more details and specifics of methods see individual papers.

Table 1: Measurement performed at study sites

Measurement	**Italy**	**Czechia**	**Israel**
Evaporation front	Yes	Yes	Yes
Tensile strength	Yes	No	Yes
Drilling resistance	No	No	Yes
Suction pressure	No	Yes	No
Moisture content	No	Yes	No
Infiltration rate	Yes	Yes	Yes
Salt composition	Yes	No	Yes
Pore size distribution	Yes	Yes	No
Hydraulic conductivity	Yes	Yes	No
Water vapor diffusion coefficient	Yes	Yes	No
Retention curve	No	Yes	No

Results and discussion

In this chapter, the results from individual papers are compared. More detailed information is in the papers itself.

Field measurements

The depth of the evaporation front

The evaporation front showed similar behavior on cavernous forms in Italy and Czechia, while it was very different in arid environments in Israel. The depth of the evaporation front varied from the surface to a maximum depth of 17 mm for coastal honeycombs in Italy and 19 mm for tafoni in Czechia. In the case of Israel, the evaporation front in inland notches in the Mediterranean climate was also at most a few millimeters below the surface, but in tafoni in semiarid to hyperarid environments, it extended to depths of hundreds of millimeters, often beyond the probe's reach.

The tensile strength

The tensile strength of coastal honeycombs in Italy was 354 kPa on average inside the honeycomb and 284 kPa outside and there is thus no significant difference between these two types of surfaces. On, the contrary the strength of the limestone in Israel is significantly reduced inside the caverns, ranging up to tens of kPa, while on outside surfaces it reaches thousands of kPa. This indicates a significant reduction in strength by salt weathering in caverns in Israel, which is not present in the coastal honeycombs in Italy, probably due to the regular and intensive removal of weathered material by the surf. In Israel, no external forces are acting on the caverns, so the weathered material remains in situ until its failure under its own weight by gravity forces. The maximum strength is higher for limestone by about one order of magnitude, which is most

likely due to the higher strength of the original unweathered material. However, the reduction in strength of coastal honeycombs due to higher moisture content may also play a role. In Kralupy site in Czech the tensile strength was not measured.

Drilling resistance

The depth of the drilled hole, which due to its destructiveness was measured only in Israel sites ranged from 1 to 12 mm (Fig. 7). The depth of the drilled hole was consistently higher inside the cavities compared to the outside surfaces, across all sites. Thus, cavities were more weathered. The most significant difference between drilled depths inside and outside was at study sites with tafoni. On the other hand, on the study site with inland notches, the difference between drilled depths inside and outside was almost negligible. This agrees with the findings of tensile strength.

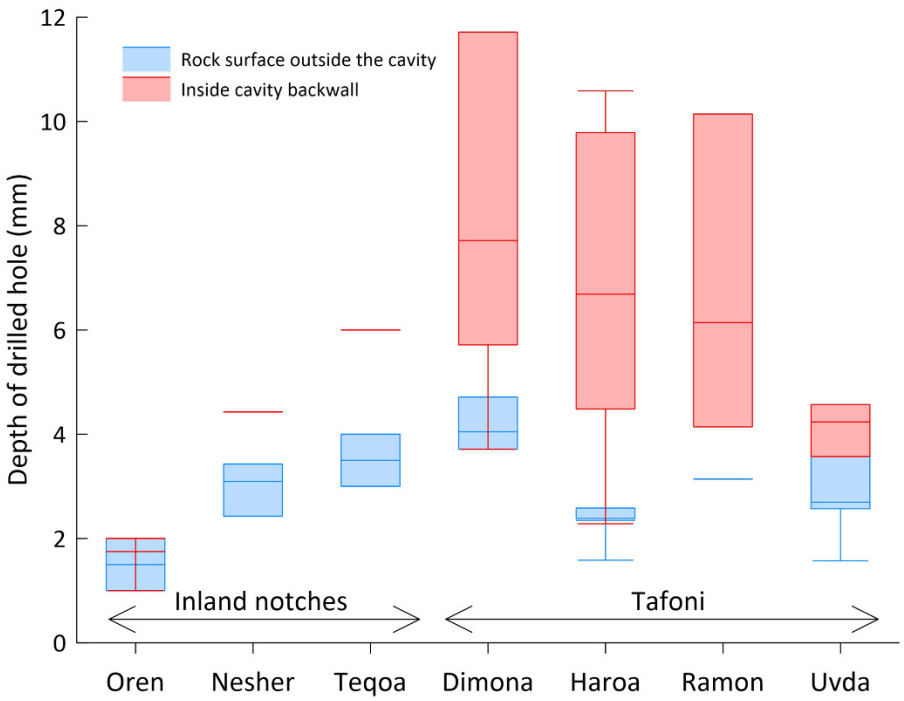

Figure 7: Depth of drilled holes measured at all sites. The center line represents the mean value, the box edges represent the first and third quartiles, and the horizontal lines represent the

minimum and maximum values. Singular horizontal lines are the result of a single measurement (Mareš et al., 2024a).

Suction pressure ranged from 25 to >100 kPa. Lower suction pressure corresponds to higher moisture content and vice versa. suction pressure shows a clear seasonal variation with high moisture content in spring and low in summer (Fig. 8). High suction pressures in the shallow hole on the outer surface indicated that the capillary connection had been lost, so the depth of the evaporation front was beyond the bottom of the hole at these times. T5x tensiometers were found to lose hydraulic connection in arcosic sandstone boreholes in the field when suction exceeded approximately 80 kPa, so measurements were stopped around these values. Suction pressures in the measured range of 80–100 kPa may therefore have been even higher in reality.

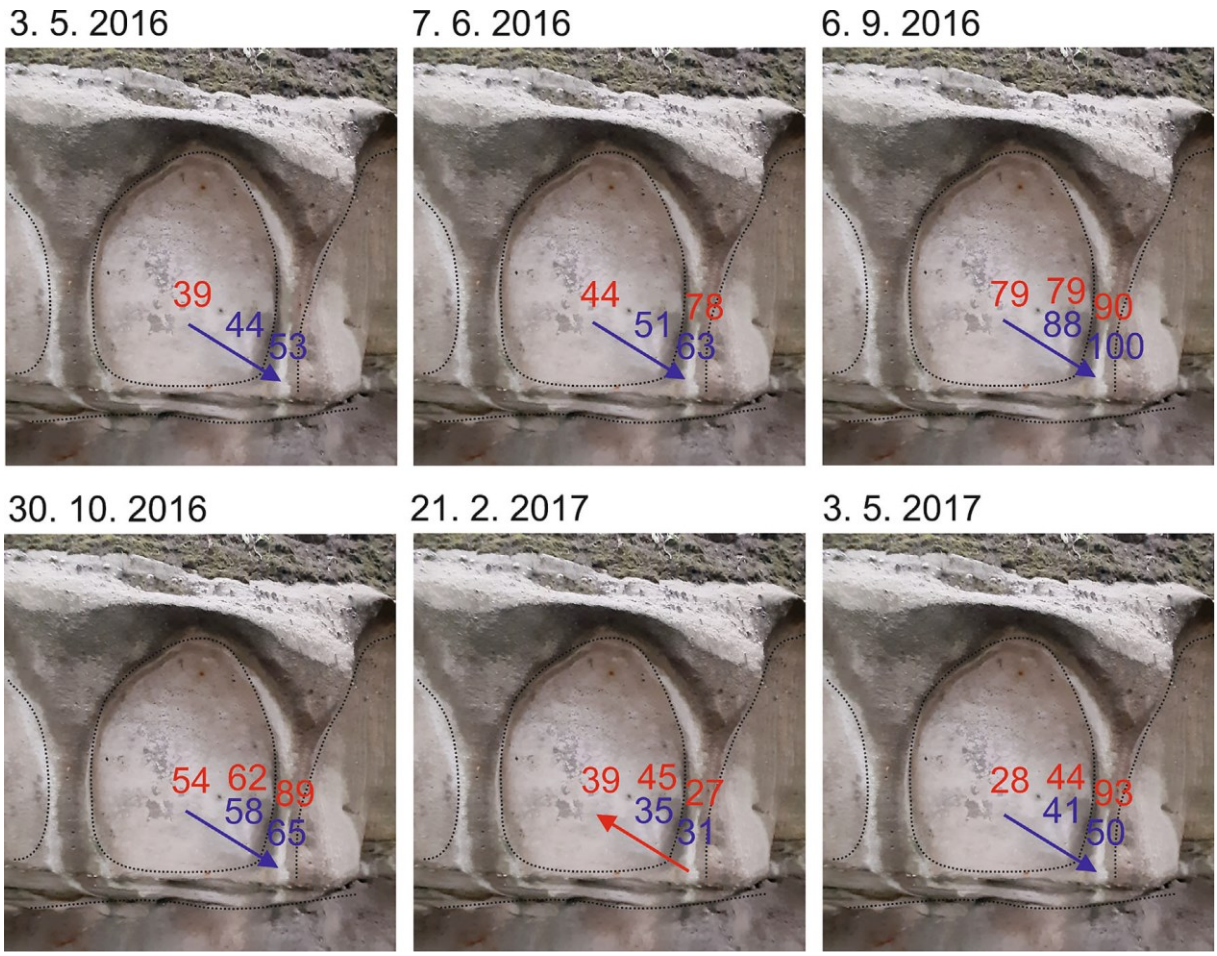

Figure 8: Suction pressure in the tafone on selected dates. Red numbers indicate shallow holes, while blue numbers represent deep holes. The blue arrow indicates moisture flux from the cavern to the outer surface; the red arrow indicates moisture flux from the outer surface to the cavern (Mareš et al., 2024b).

Moisture content

The TDR measurements showed that the moisture content in Czechia increased from the surface to a depth of 75 cm. It was from 6%–9% at the surface to 16% in depth in both the outer surface and the cavern (Fig. 9). In depth exceeding 60 cm, the moisture content was constant with depth and the same below the cavern and outer surface. This indicates the flow of liquid water from the rock interior towards the rock surface. Due to the high cost of the TDR probe, the moisture content was not measured at foreign sites.

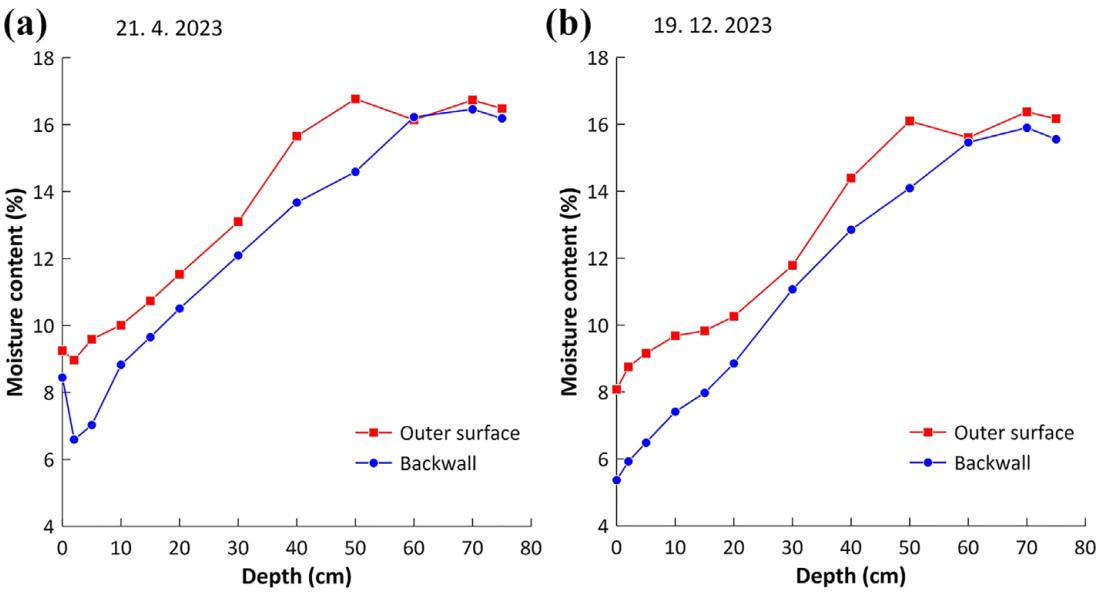

Figure 9: Increasing moisture content with depth below the tafone surface measured by TDR on 21.4.2023 and 19.12.2023 (Mareš et al., 2024b).

The infiltration rate

Infiltration rate in Israel ranged from 8×10^{-3} to 1.3×10^{-6} m/s inside the caverns, while outside it ranged from 4.2×10^{-7} to 1.7×10^{-8} m/s. The honeycombs in Italy did not allow measurements inside due to too high curvature of surfaces, and the values outside show that the infiltration rate was around 4×10^{-9} m/s. This indicates that it is orders of magnitude more difficult for water to infiltrate the metasandstone than the unweathered limestone in Israel. The infiltration experiment in Czechia showed that the infiltration rate into the outer surface of the tafoni was 1×10^{-7} m/s, which is similar to the limestones in Israel.

The salt composition

The concentration of salts ranged from 0.7 to 1.5 wt.% in Italy and from 0.6 to 7 wt.% in Israel. In Czechia, it was from 0.2 to 9 wt.% (Karatas et al., 2022). In Israel, such high concentrations were achieved only in tafoni (up to 7 wt. % inside the cavities), while inland notches had concentrations significantly lower (0.6–1.3 wt. %). The higher concentrations in the tafoni in Israel are mainly due to the existence of a weathered layer, which has the highest concentrations of salts, and which in Italy is regularly removed by the surf, while in Israel it remains in situ. In both Italy and Israel, the dominant salt is NaCl.

Laboratory measurements

Evaporation experiment

At the beginning of the evaporation experiment, the block with coastal honeycombs was drying rapidly, losing almost 50% of the moisture content in 24 h (phase I. in Figure 10). During this phase, the evaporation front in the honeycomb lips retreated into the block much faster than in

the pits (16 mm and 2 mm by the end of phase I., respectively) and even remained at the surface in the case of some pits. Over the next 3 days, the evaporation front depth kept rapidly increasing by _2–3 mm/d for both pits and lips; but after the fourth day slowed down to values <1 mm/d. After phase I. of the rapid evaporation, a dynamic balance between the inflow of water from the cotton cloth and outflow by evaporation was attained (phase II. in Figure 10). The small apparent increase in moisture content is most likely caused by the precipitation of salts, which increased the weight of the block and affected the measurement. After 10 days, water in the reservoir below the block was depleted, and the entire block dried up (phase III. in Figure 10). Relative surface moisture values correspond to the evaporation front depth – a fast decrease at the beginning of the drying, followed by a slowdown. After 24 h, the mean relative surface moisture in the honeycomb lips declined to 10, which is the value for a surface of dry material. This value in the pits was reached after 14 days, also pointing to the faster drying in the lips.

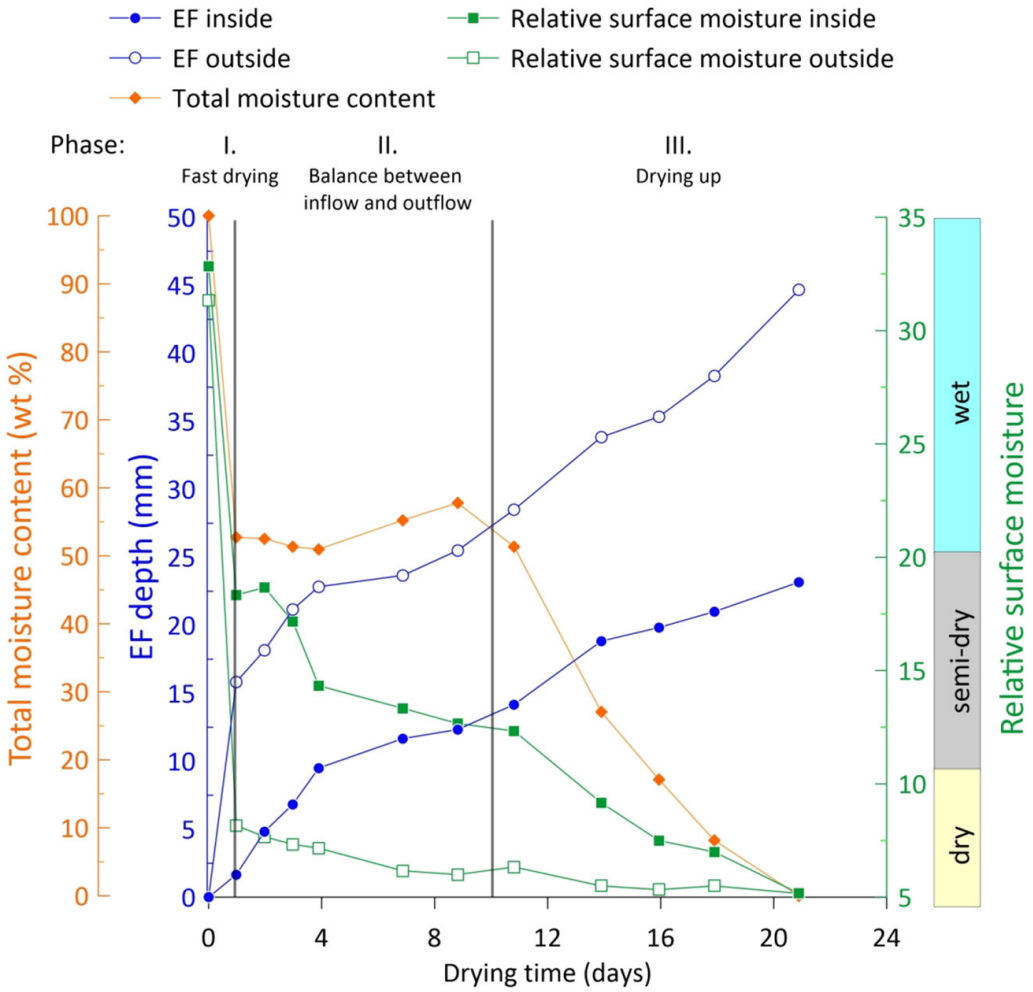

Figure 10: The evaporation front (EF) depth, relative surface moisture, and total moisture content of the block of Italy metasandstone with honeycombs during the evaporation experiment (Mareš et al., 2022).

Pore size distribution

The porosity of arcosic sandstone in Czechia is significantly higher than that of metasandstone in Italy. While the measured porosity in Czechia is around 22%, in Italy it is only 7% (Fig. 11). This is due to filling the pores during metamorphoses in the case of the Italian sample. The abundance of micropores, which are essential for salt weathering (Yu and Oguchi, 2010), also differs. The metasandstone in Italy has <5 um pores up to 79%, so in Czechia, the arcosic

sandstone has these pores only up to 59%. The Italian metasandstone has micropores <0.1 um up to 17%, while the Czech arcosic sandstone has only 8%. This suggests that the Italian metasandstone is more susceptible to salt weathering. Porosity in Israel was not studied due to financial reasons.

a

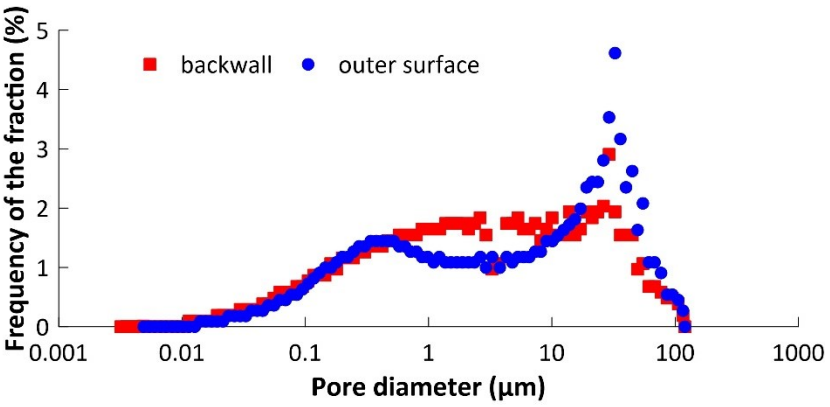

.

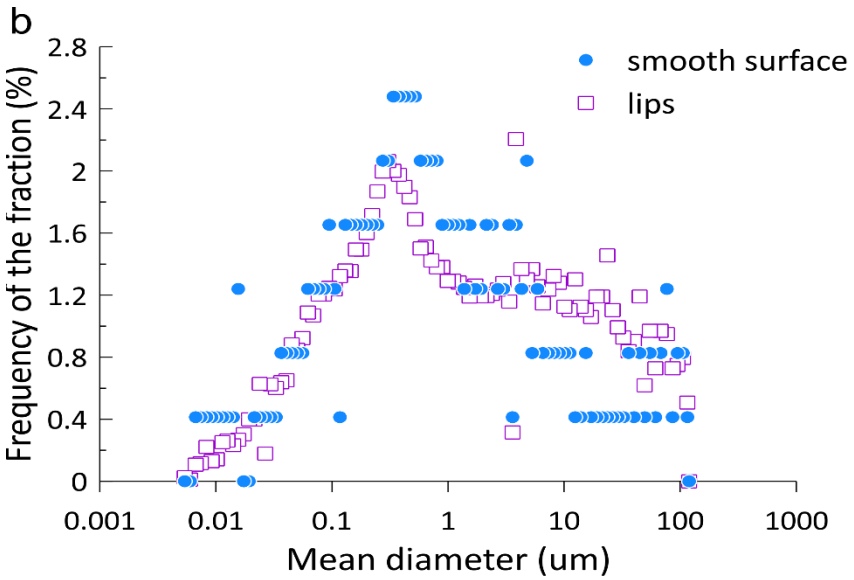

Figure 11: Pore size distribution of a) arcosic sandstone from Czechia (Mareš et al., 2024b) and b) metasandstone from Italy (Mareš et al., 2022).

Retention curve

Figure 12 shows the relationship between moisture content and suction pressure for samples from arcosic sandstone from Czechia and the fitted model retention curves. Samples O1, O3, and B1 correspond to surface material with salts. Samples B2 and O2 were leached several times with water before the retention curve was measured and correspond to the material below the evaporation front without salts. Retention curves of rock with leached salt have steeper slopes in the first phase. The retention curve of studied arcosic sandstone falls between curves typical for sand and silt.

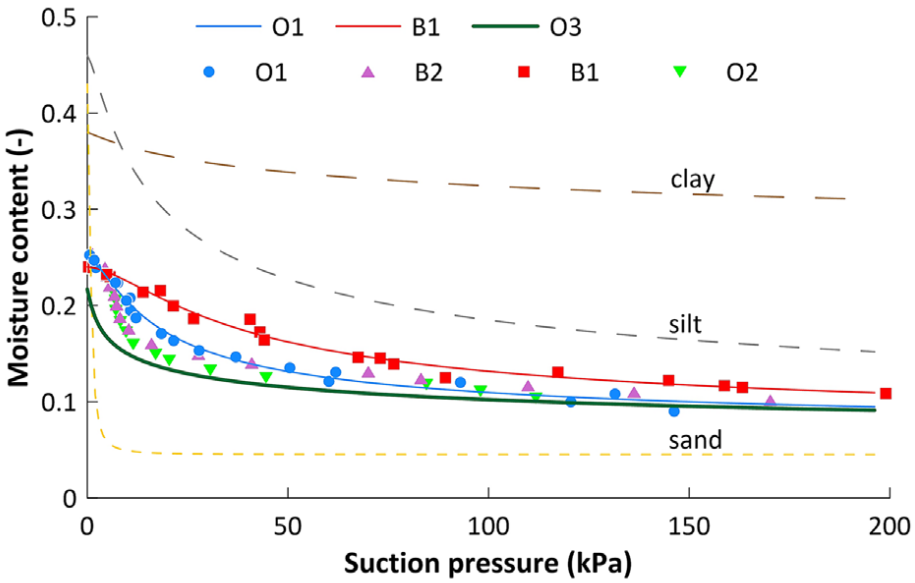

Figure 12: Measured retention curve data (points), fitted model retention curves, and typical retention curves for sand, silt, and clay; the samples collected from the cavern of the tafone are marked as "B" and those from the outer surface as "O" (Mareš et al., 2024b).

Water vapor diffusion coefficient

The water vapor diffusion coefficient of the metasandstone in Italy was 5.4×10^{-12} s. The water vapor diffusion coefficients of the inner and outer surface of the arcosic sandstone in Czechia were 3.1×10^{-11} s and 2.7×10^{-11} s respectively. It shows that arcosic sandstone in Czechia is in order of magnitude more permeable than water vapor than metasandstone in Italy.

Hydraulic conductivity

The saturated hydraulic conductivity inside the cavity of the Czechia arcosic sandstone was 5×10^{-7} m/s and outside it was 1×10^{-7} m/s. This is consistent with observations by Studencová (2017) from other localities with tafoni occurrence. The higher hydraulic conductivity is probably caused by the absence of biocrust in the cavern, which is clogged by fines transported by the overland flow and infiltrated to the outer surface. The hydraulic conductivity of the Italian metasandstone was 3×10^{-12} m/s, which is five orders of magnitude lower than that of the Czech arcosic sandstone. This is due to filling the pores during metamorphoses in the case of the Italian sample.

Summary and outlook

This PhD thesis summarizes three publications on moisture measurements in rock outcrops with cavernous weathering. The first site consisted of metasandstones with honeycombs on the Mediterranean coast (Italy; Mareš et al., 2022), the second was in carbonates across climatic zones in Israel where distinct cavernous forms occur (Mareš et al., 2024a), and the third was in arkosic sandstone with tafoni in a humid climate near Kralupy nad Vltavou, Czechia (Mareš et al., 2024b). Moisture characteristics were measured at all study sites, and strength characteristics were measured at selected sites.

The evaporation front was closer to the surface inside the caverns than outside most of the time at the tafoni and honeycombs sites. In the case of Israel, the evaporation front was mostly directly at the surface in inland notches, and the average depth increases with decreasing annual precipitation. In coastal honeycombs and humid tafoni, the evaporation front was on average a few millimeters below the surface and the difference between inside and outside surfaces was rather small, yet still significant in providing higher evaporation rate inside cavities and thus higher salt deposition there compared to outer surfaces. But in the tafoni in semi-arid to hyperarid areas of Israel the evaporation front was hundreds of millimeters deep and often deeper than the probe used, which length was 320 mm. However, during measurement in 2023, the evaporation front was exceptionally detected closer to the surface outside the caverns, a consequence of the precipitation event that preceded the measurement. This shows a different regime where in humid and coastal areas water recharge is more frequent and thus the capillary front is found close to the rock surface and the evaporation front does not retreat significantly below the rock surface. In arid regions, on the other hand, there are long intervals between individual recharge events, resulting in the drying of the outcrop to a depth of tens or hundreds of millimeters.

The evaporation experiment with coastal honeycombs showed that during the first phase of evaporation, the weight of the block dropped rapidly as about 45% of the water evaporated. The evaporation front dropped to a depth of about 10 mm in the honeycomb pits and 20 mm on the walls separating the pits. In the second phase, an equilibrium was reached between the evaporated water and the supply from the interior of the rock (represented by the wet cotton), where neither the weight nor the depth of the evaporation front decreased significantly with time. After ten days, a third phase occurred when the water supply from the interior was exhausted, and the block gradually dried out completely. It shows that during evaporation, the honeycomb lips dry first, and the pits remain wet for a longer time, so the evaporation rate is higher from the pits. This is consistent with the theory of salt weathering that pits obtain more water and thus precipitate salt and thus more intense salt weathering (Huining et al., 2004; Bruthans et al., 2018; Safonov and Minchenkov, 2023).

Tensile strength has been measured on coastal honeycombs in Italy and on carbonates in different climatic zones in Israel. While the strength inside and outside the cavities (pits) in the metasandstones with honeycombs in Italy is practically the same, cavernous weathering in Israel is characterized by a significant decrease in strength inside the cavities. In the inland notches, the strength is reduced by about an order of magnitude compared to the outer surface; in the tafoni, the strength is as high outside, but inside it significantly drops due to salt weathering. Such a significant difference is probably because in Israel the weathered material is not exposed to significant external forces, which would cause its removal. In Italy, on the other hand, all the weathered material is swiftly removed away by the surf. The measurements show that the study of moisture and strength properties allows a detailed description and quantification of weathering in cavernous weathering forms.

Samples of drilled material were taken from honeycombs in Italy and from inland notches and tafoni in Israel to determine the concentration and composition of salts. The concentrations

ranged from 0.7 to 1.5 wt% in Italy, from 0.4 to 7.3 wt% in Israel. The salt concentration in Czechia ranged from 0.2 to 9 wt.% (Karatas et al., 2022). The dominant salt in Italy and Israel is halite and in Czechia is gypsum. Both honeycombs and tafoni showed similar concentrations but salt concentrations in the inland notches are significantly lower. This is due to different types of weathering, the honeycombs and tafoni being formed by salt weathering and the inland notches by karstification (limestone dissolution).

For the first time, the evaporation rate and the amount of precipitated salts were quantified. Based on the evaporation rate, the water balance for the rock outcrop in Czechia was calculated. In Czechia, the main sources of water for tafone are the influx of water from the interior of the rock and the infiltration of overland flow after heavy rainfall. The infiltration rate of overland flow to the outer surfaces of the tafone was determined from infiltration experiments to be 10 mm/day when overland flow is active. The input from the condensation of the air humidity was 0.7 kg/m^2/year. Evaporation is the only process by which water leaves the tafone. In Czech tafoni, the evaporation rate ranges from 300 mm/year in summer to less than 15 mm/year in winter, with an average of 62 mm/year inside the caverns and 46 mm/year outside (Fig. 13). In Italy coastal honeycombs, the evaporation rate inside the caverns is 16.1 mm/year and 4.6 mm/year outside. At this rate, 650 g/m^2/year of salts are precipitated inside the caverns, and 190 g/m^2/year of salts outside the honeycomb caverns. Salt precipitation in Czech tafoni averages 13 g/m^2/year inside and 11 /m^2/year outside. The higher evaporation rate in Czech tafoni is mainly due to the different relative humidity at the evaporation front caused by the different occurrence of deliquescent salts, which is RH 85% in Czechia and 75% in Italy. Nevertheless, due to the significantly higher mineralization of the evaporated water (marine water in Italy), more salts are precipitated in Italy than in Czechia. This shows that a higher temperature does not necessarily mean a higher evaporation rate and a higher evaporation rate does not necessarily mean a high deposition rate of salts. Hence, salt deposition rates are not trivial and

need to be properly calculated based on data measured in the field. For the first time, moisture fluxes and the water balance of the rock outcrop with cavernous weathering forms have been determined. This allows the water balance of other rock outcrops to be determined and the relative rate, intensity, and location of weathering to be predicted in the future.

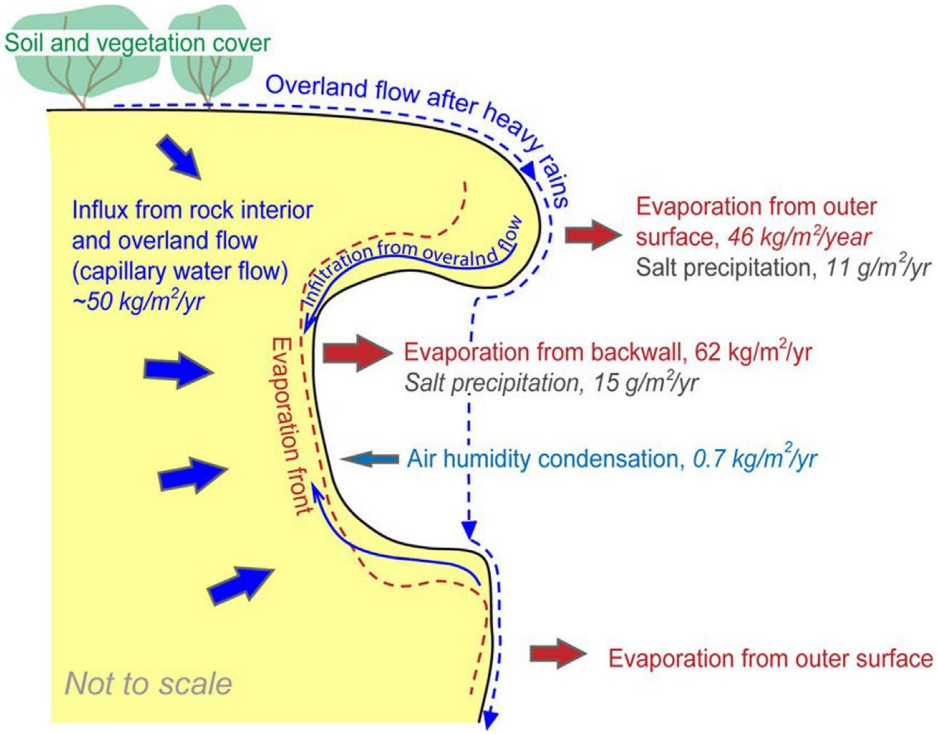

Figure 13: Schematic model showing water balance of outcrop with tafoni. Blue arrows represent influx, and red lines represent outflux. Evaporation and air humidity condensation represent vapor flow. The position of the evaporation front is only approximate as it fluctuates in time (Mareš et al., 2024b).

Figure 14 shows that the evaporation rates in caverns and outer surfaces differ greatly at individual tafoni and honeycomb sites. At some sites, the evaporation rate from caverns is up to 2 orders of magnitude higher than from outer surfaces, due to a much shallower evaporation front in caverns compared to outer surfaces (mainly at arid and semi-arid sites). However, at temperate and coastal sites, the evaporation rate on caverns and outer surfaces is comparable

due to a small difference in the depth of the evaporation front on caverns and outer surfaces. This indicates that in arid and semi-arid sites, much more salt is deposited on caverns than on outer surfaces, whereas in temperate and coastal settings, the difference in salt deposition is smaller. The relatively small difference in evaporation rate and consequently salt deposition rate between caverns and outer surfaces in temperate climate makes tafoni and honeycombs more vulnerable to destruction in this climatic setting. Even a small increase in water influx can shift the dominant salt deposition from the caverns to the outer surfaces and thus initiate tafoni degradation (Safonov and Minchenkov, 2023). This is indeed visible in Czechia where in some places the tafoni outer surfaces are degrading, while in other places tafoni are evolving. However, this markedly different hydrological regime (in the humid climate) is still producing similar forms (tafoni and honeycombs) as in the arid climate.

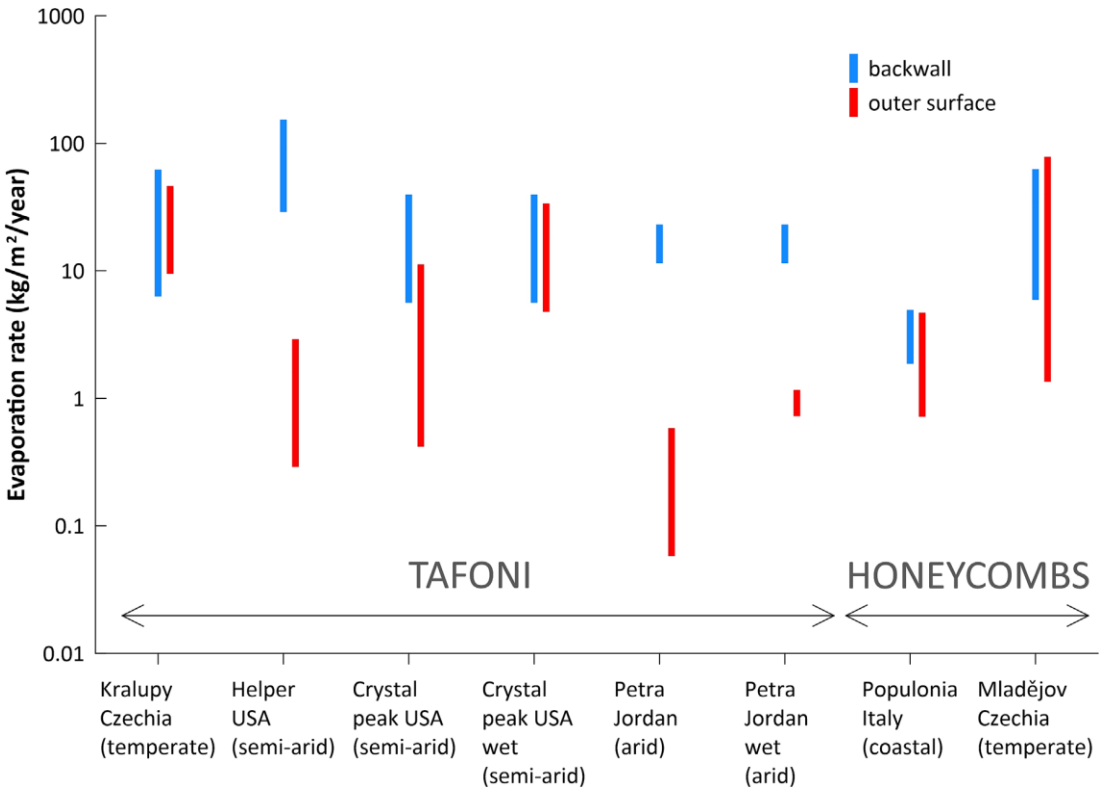

Figure 14: Comparison of evaporation rates from different locations of tafone and honeycombs separately for caverns (backwalls) and outer surfaces. Evaporation rates were calculated from measured capillary front depths (Bruthans et al., 2018; Karatas et al., 2022), air humidity, and

temperature logs for given sites and measured vapor diffusivity coefficients for given rocks from Slavík et al. (2023; Mareš et al., 2024b).

This thesis shows that moisture can be measured in different lithologies, such as sandstone, limestone, or metamorphic sandstone. The suite of measurement techniques is capable of characterizing spatial and temporal moisture changes and quantifying moisture fluxes and salt deposition rates in different parts of the cavernous weathering forms and other granular rock landforms to better understand the processes controlling weathering, epi/endolithic life, water balance and to test various hypotheses. These techniques are labor-intensive but provide similarly deep insight into moisture patterns and salt transport as the established soil hydrology techniques. Calculation of the evaporation rate and the amount of precipitated salts allows quantification of salt weathering and helps predict salt weathering damage not only to natural outcrops but also to historic buildings.

Summary of the individual articles

Coastal honeycombs (Tuscany, Italy): Moisture distribution, evaporation rate, tensile strength, and origin

This paper uses field and laboratory measurements to describe the moisture and strength of metasandstones with honeycomb from the Mediterranean coast of Italy. During the summer, the depth of the evaporation front was measured at 10 locations inside the honeycombs and at 12 walls separating the honeycombs. The evaporation front in honeycombs less than 1 m above the high tide line is always at the surface both in the pits (caverns) and on the lips. The depth varies from 0 to 17 mm. In all honeycombs, the evaporation front is deeper in the lips than in the pits. Furthermore, the measured depths of the evaporation front were compared with the depth of the honeycombs. The results show that the evaporation front is not straight but weakly follows the surface. Tensile strength was also measured in 5 pits and 6 lips. The average values are not significantly different (354 kPa in the pits and 284 kPa in the lips), so case hardening is not present, and weathered material from the pits is probably periodically removed by the surf.

In the laboratory, the composition of the collected salts was analyzed, and the hydraulic properties of the material were measured - porosity, hydraulic conductivity, capillary water absorption, and diffusion coefficient. The salts range in concentration from 0.7 to 1.5 weight percent. The dominant salt is halite. Porosity ranges from 6 to 7%. Most of the pore diameters are less than 5 μm, indicating a high susceptibility of the rocks to salt weathering. The hydraulic conductivity of the metasandstone is 3×10^{-12} m/s and the diffusion coefficient is 5.4×10^{-12} s, indicating very low permeability to both liquid water and water vapor. Slavík (2020) measured these parameters for quartz sandstones in the Bohemian Paradise, which also contain honeycombs, and found 7 orders of magnitude higher hydraulic conductivity and an order of

magnitude higher diffusivity and porosity coefficient of 30%. Capillary water absorption ranges from 0.3 kg/m^2/h for flow perpendicular to the layers to 0.6 kg/m^2/h for flow parallel to the layers.

A laboratory experiment was also conducted in which a block of honeycomb was saturated with salt water and allowed to evaporate under the conditions of a hot Mediterranean summer. During evaporation, the block was periodically weighed and the depth of the evaporation front in the pits and at the lips was measured. During the first phase of evaporation, the weight of the block dropped rapidly as about 45% of the water evaporated. The evaporation front dropped to a depth of about 10 mm in the pits and 20 mm on the lips. In the second phase, an equilibrium was reached between the evaporated water and the supply from the interior of the rock (represented by the wet cotton), where neither the weight nor the depth of the evaporation front decreased significantly with time. After ten days, a third phase occurred when the water supply from the diaper was exhausted, and the block gradually dried out completely.

Based on the measured depth of the evaporation front, the evaporation rate and the amount of precipitated salts were calculated for the pits and lips. The evaporation rate is 16.1 kg/m^2/year for the pits and 4.6 kg/m^2/year for the lips. At this evaporation rate, the pits precipitate 650 g/m^2/year of salts (of which 560 g/m^2/year of halite) and the lips 190 /m^2/year of salts (of which 160 g/m^2/year of halite).

This paper describes the moisture distribution in coastal honeycombs and calculates evaporation and salt precipitation rates. The evaporation front is closer to the surface in the pits than on the lips, leading to a higher evaporation rate and greater salt precipitation in pits, results were confirmed by evaporation experiments under laboratory conditions. This work contributes to the understanding of the origin of cavernous weathering in coastal areas and builds on

previous theoretical work (Huinink et al., 2004) and measurements in the Bohemian Paradise, Czechia (Bruthans et al., 2018).

For the first time, this study calculates the evaporation rate from a natural honeycomb outcrop based on the depth of the evaporation front, the diffusivity coefficient, and climatic conditions. The amount of precipitated salts was determined from the evaporation rate and mineralization of the evaporated water. The results show that coastal honeycombs in the Mediterranean are formed by the same mechanism as honeycombs in the humid climate of Bohemian Paradise, Czechia.

Climate controls on limestone cavernous weathering patterns in Israel

A significant climatic gradient exists in Israel over a relatively short distance, where the west coast has a Mediterranean climate with an annual rainfall of 600 mm, transitioning to a hyper-arid desert environment with annual rainfall of less than 20 mm. In this environment, there are carbonate outcrops with various forms of cavernous weathering (tafoni and inland notches). Moisture and strength properties were measured on these forms, both inside the forms and on their outer surfaces.

Seven sites were selected, three with inland notches and four with tafoni. Inland notches were monitored at the Oren and Nesher sites in the Mount Carmel area with an annual rainfall of 600 mm and at the Teqoa site with an annual rainfall of 300 mm. Tafoni was studied at the Dimona, Haroa, Ramon, and Uvda sites. Rainfall has been gradually decreasing at these sites, with 150 mm/year at Dimona, 90 mm/year at Haroa, 50 mm/year at Ramon, and 20 mm/year at Uvda.

The first characteristic observed was the depth of the evaporation front. While at the inland notches sites, the evaporation front was mostly at the surface, at the tafoni sites the evaporation front was deep below the surface, often below the level of the uranine-probe reach. The average depth of the evaporation front increases with decreasing annual precipitation. Typically, the evaporation front is deeper below the outer surfaces and closer to the surface in the tafoni caverns. In 2023, the evaporation front was exceptionally detected closer to the surface outside the caverns, a consequence of the precipitation event that preceded the measurement.

At all sites, lower tensile strength was measured inside the caverns than outside. The tensile strength of the unweathered surface outside the caverns is approximately the same at all sites, reaching up to 6 MPa. Inside, the highest average strength values were measured at the Nesher site, where they reached 380 kPa, and dropped to 0.1 kPa at the tafoni sites. Drilling resistance measurements gave similar results. All sites have more weathered (softer) rock inside the

caverns according to the drilling resistance, but this difference is more pronounced at the tafoni sites. The weathered surface of the caverns also affects the infiltration rate. It is always higher inside the caverns than on the outer surfaces. Inside the caverns, it is in the order of 10^{-3}-10^{-6} m/s, while on the outer surfaces, it is 10^{-7}-10^{-8} m/s, regardless of the form of weathering.

In addition, salts from different depths inside and outside the caverns were collected and analyzed at all sites according to the methodology of Karatas et al. (2022). The measured salt concentrations range from 0.4 to 7.3 wt%. At inland notch sites, salt concentrations are very low and there is no significant difference with either depth or sampling location. At the tafoni sites, there is evidence of higher salt concentrations inside the caverns than outside. While there is little difference with depth outside the cavern, inside the cavern the highest salt concentration is just below the surface and the salt concentration decreases with depth below the surface.

The availability of water is essential for the formation of individual cavern shapes. In inland notches, there is an excess of water in the environment and there is an absence of salt weathering. Karstification is the dominant process. In tafoni, on the other hand, water is scarce, and salt crystallizes below the rock surface and salt weathering occurs. This results in a significant reduction in the strength of the caverns compared to the unweathered surface. The difference in tensile strength between unweathered and weathered surfaces is up to 4 orders of magnitude. The boundary between karst weathering with inland notches and salt weathering with tafoni is in the range of annual rainfall of 250-300 mm.

Moisture patterns and fluxes in evolving tafoni developed in arkosic sandstone in temperate climate

Between Kralupy nad Vltavou and Nelahozeves, Czechia, there are outcrops of Carboniferous rocks along the Vltava River. They are one of the few places in a humid climate where tafoni are perfectly developed. The spatial and temporal distribution of moisture was measured on these tafoni and the water fluxes and hydrological balances of the tafoni were calculated from the measured values.

The depth of the evaporation front was measured at 5 points inside and 4 points outside the tafone over a period of two years with a measurement interval of about 1 month. The average evaporation front depth inside the tafone is 2.7 mm with a median of 2 mm and outside is 3.3 mm with a median of 3 mm. Usually, the evaporation front is deeper on the outer surfaces, but after the rains, the evaporation front is on the outer surface of the tafone.

Suction pressure was measured at 3 points inside and 2 outside for one year with a measurement step of about 1 month. The lowest suction pressure was 25 kPa, while the highest was over 100 kPa. The water flow based on suction pressure indicated a dominant direction of water flow from the inside of the rock mass to the outside, but after heavy rains, the flow reversed and was directed from the outside surfaces to the cavern of the tafone. Based on the knowledge of the retention curve, the moisture content was calculated from the suction pressure, which ranged from 10 to 13%.

The calculated moisture content results were then compared with direct measurements using an ultra-precise TDR. The values measured by the TDR have a wider range. The difference between the measured and calculated values is mainly due to the accuracy of the retention curve determination. However, the recalculation of the suction pressure allows a more accurate

moisture determination than conventional moisture meters based on the electrical conductivity principle. In addition, moisture determined from suction pressure allows point measurements, unlike other methods (including ultra-precise TDR).

The effect of air humidity condensation on the water source was monitored using two cores covered by epoxy on all but one side, placed in a tafone frame out of the rain, and periodically weighed. The increase in weight then corresponds to the increase in moisture due to condensation. Measurements show that water condenses into the porous environment of the tafone at an intensity of 0.7 kg/m^2/year.

In order to find out how much water infiltrates from the surface into the tafone after intense rainfall, an experiment with artificial wetting of the surface was carried out. During this experiment, 0.13 liters infiltrated into an area of 80×20 cm in two hours, indicating an infiltration rate of about 10 mm/day.

The properties of the arcosic sandstone - porosity, diffusion coefficient, and saturated hydraulic conductivity - were determined in the laboratory. The porosity inside and outside the tafone is practically the same and reaches 22%. The saturated hydraulic conductivity of the material inside the tafone is 5×10^{-7} m/s and outside 1×10^{-7} m/s, and the diffusion coefficient is 3.1×10^{-11} s inside and 2.7×10^{-11} s outside. The higher permeability inside the tafone is probably due to the absence of biocrusts inside the tafone and has been observed at other tafoni sites (Studencová, 2017).

The measurements show that the evaporation front is deeper inside the tafone cavity than below the outer surface most of the time. Based on the measured evaporation front depths and suction pressure, water fluxes were determined and a water balance of the tafoni outcrop was constructed. Evaporation ranges from 300 kg/m^2/year in summer to less than 15 kg/m^2/year in winter. The mean evaporation rate from the cavern was 62 kg/m^2/year and from the outer

surface was 46 kg/m^2/year. The influxes to the tafone were calculated to be 50 kg/m^2/year and 0.7 kg/m^2/year from air humidity condensation. The evaporation rate was compared between different cavernous weathering sites. Tafoni in humid climates show less difference between the depth of the evaporation front inside and outside, making them more susceptible to degradation and smoothening of the surface.

References

Allan R.G., Pereira L.S., Raes D., Smith M. (1998) Crop evapotranspiration-Guidelines for computing crop water requirements-FAO Irrigation and drainage paper 56. B.m.: FAO - Food and Agriculture Organization of the United Nations. 300 str. ISBN 92-5-104219-5.

Angerer L. and Birle E. (2016) Experimental determination of the hysteretic behaviour of soil-water retention curve of silty sands. E3S Web of Conferences 9, 11004.

André M.F. and Hall K. (2005) Honeycomb development on Alexander Island, glacial history of George VI Sound and palaeoclimatic implications (Two Step Cliffs/Mars Oasis, W Antarctica). Geomorphology 65, 117–138.

Brandmeier M., Kuhlemann J., Krumrei I., Kappler A., Kubik P.W. (2011) New challenges for tafoni research. A new approach to understand processes and weathering rates. Earth Surface Processes and Landforms, 36(6), 839–852.

Bruthans J., Svetlik D., Soukup J., Schweigstillova J., Valek J., Sedlackova M., Mayo A.L. (2012) Fast evolving conduits in clay-bonded sandstone: Characterization, erosion processes and significance for the origin of sandstone landforms. Geomorphology, 177, 178-193.

Bruthans J., Soukup J., Vaculikova J., Filippi M., Schweigstillova J., Mayo A.L., Masin D., Kletetschka G., Rihosek J. (2014) Sandstone landforms shaped by negative feedback between stress and erosion, Nat. Geosci., 7, 597–601.

Bruthans J., Filippi M., Slavík M. and Svobodová E. (2018) Origin of honeycombs: Testing the hydraulic and case hardening hypotheses. Geomorphology 303: 68–83.

Buckingham E. (1907) Studies on soil moisture movement. US Dept. Agr. Bur., Soil Bul., 38.

Churayev N.V., Rode L.G. (1966) Measuring the moisture content of organic peat soils by the neutron method, Pochvovedenie, 1, 96-100.

Conca J.L. and Rossman G.R. (1982) Case hardening of sandstone. Geology 10, 520–523.

Fick A. (1855) Ueber Diffusion. Annalen der Physik. 170(1), 59–86.

Gavilán P., Castillo-Llanque F. (2009) Estimating reference evapotranspiration with atmometers in a semiarid environment. Agricultural Water Management. 96(3), 465–472.

Goudie A.S., Migoń P., Allison R., Rosser N. (2002) Sandstone geomorphology of the Al-Quwayra area of south Jordan. Zeitschrift für Geomorphologie, 46(3), 365–390.

Gregory K.J., Goudie A. (2011) Introduction to the discipline of geomorphology. The SAGE Handbook of Geomorphology. London: SAGE, 1-20.

Hendrickx R. (2013). Using the Karsten tube to estimate water transport parameters of porous building materials: The possibilities of analytical and numerical solutions. Materials and structures, 46, 1309-1320.

Hillel D. (2004) Introduction to Environmental Soil Physics. Elsevier Academic Press, Amsterdam.

Huinink H.P., Pel L. and Kopinga, K. (2004) Simulating the growth of tafoni. Earth Surface Processes and Landforms 29, 1225–1233.

Idso S.B., Reginato R.J., Jackson R.D., Kimball B.A., Nakayama F.S. (1974) The three stages of drying of a field soil1. Soil Sci. Soc. Am. J. 38, 831.

Karatas T., Bruthans J., Filippi M., Mazancová A., Weiss T. and Mareš J. (2022) Depth distribution and chemistry of salts as factors controlling tafoni and honeycombs development. Geomorphology 414, 108374.

Lehmann P., Assouline S., Or D. (2008) Characteristic lengths affecting evaporative drying of porous media. Physical Review E. 77(5), 056309.

Maľa M. and Greif V. (2021) Effect of frost damage on the pore interconnectivity of porous rocks by spontaneous imbibition method. Bulletin of Engineering Geology and the Environment, 80, 8789-8799.

Manning, J.C. (2016) Applied Principles of Hydrology: Third Edition. B.m.: Waveland Press, Inc. 276 p.

Mareš J., Bruthans J., Weiss T., Filippi M. (2022) Coastal honeycombs (Tuscany, Italy): Moisture distribution, evaporation rate, tensile strength, and origin. Earth Surface Processes and Landforms, 47(6), 1653-1667.

Mareš J., Weiss T., Wieler N., Shtober-Zisu N. (2024a) Climate controls on limestone cavernous weathering patterns in Israel. Geomorphology, 109334.

Mareš J., Bruthans J., Studencová A., Filippi M. (2024b) Moisture patterns and fluxes in evolving tafoni developed in arkosic sandstone in temperate climate. Earth Surface Processes and Landforms, 1–15.

Matsuoka N. and Murton J. (2008) Frost Weathering: Recent Advances and Future Directions. Permafrost and periglacial processes 19, 195–210.

McBride E.F. and Picard M.D. (2000) Origin and development of tafoni in tunnel spring tuff, Crystal Peak, Utah, USA. Earth Surface Processes and Landforms 25, 869–879.

Mottershead D.N. (1994) Spatial variations in intensity of alveolar weathering of a dated sandstone structure in a coastal environment, Weston-super-Mare, UK. In Rock Weathering and Landform Evolution, Robinson DA, Williams RBG (eds). John Wiley & Sons: Chichester, 151–174.

Mustoe G.E. (1982) The origin of honeycomb weathering. Geological Society of America Bulletin 93, 108–115.

Or D., Lehmann P., Shahraeeni E., Shokri N. (2013) Advances in soil evaporation physics—a review. Vadose Zo. J. 12.

Pavlík Z., Michálek P., Pavlíková M., Kopecká I. and Maxová I. (2008) Water and salt transport and storage properties of Mšené Sandstone. Construction and Building Materials 22, 1736–1748.

Rodriguez-Navarro C., Doehme E. and Sebastian E. (1999) Origins of honeycomb weathering: the role of salts and wind. GSA Bull. 111 (8), 1250–1255.

Safonov A. and Minchenkov K. (2023) Mathematical Simulation of Honeycomb Weathering via Moisture Transport and Salt Deposition. Geosciences 13 (6), 161.

Schnepfleitner H., Sass O., Fruhmann S., Viles H. and Goudie A. (2016) A multi-method investigation of temperature, moisture and salt dynamics in tafoni (Tafraute, Morocco). Earth Surface Processes and Landforms 41: 473–485.

Shtober-Zisu N., Amasha H., Frumkin A. (2015) Inland notches: Implications for subaerial formation of karstic landforms—An example from the carbonate slopes of Mt. Carmel, Israel. Geomorphology, 229, 85-99.

Shtober-Zisu N., Amasha H., Frumkin A. (2017) Inland notches: lithological characteristics and climatic implications of subaerial cavernous landforms in Israel. Earth Surface Processes and Landforms, 42(12), 1820-1832.

Shtober-Zisu N., Vaks A., Korngreen D., Frumkin A. (2020) Slope retreat rates estimated from chronology of tufa deposits sheltered by inland notches on Mt. Carmel, Israel. Geomorphology 367, 107319.

Smugge T. J., Jackson T. J., McKim H. L. (1980) Survey of Methods for Soil Moisture Determination. Water Resources Research 16 (6), 961-979.

Slavík M. (2020) Moisture characteristics of natural sandstone exposures. PhD thesis, Charles University, Prague (in Czech).

Slavík M., Bruthans J., Filippi M., Schweigstillová J., Falteisek L. and Řihošek J. (2017) Biologically-initiated rock crust on sandstone: mechanical and hydraulic properties and resistance to erosion. Geomorphology 278, 298–313.

Slavík M., Bruthans J., Weiss T. and Schweigstillová J. (2020) Measurements and calculations of seasonal evaporation rate from bare sandstone surfaces: Implications for rock weathering. Earth Surf. Process. Landforms 45, 2965–2981.

Slavík M., Bruthans J. and Schweigstillová J. (2023) Evaporation rate from surfaces of various granular rocks: Comparison of measured and calculated values. Science of the Total Environment 856, 159114.

Studencová A. (2017) Comparison of hydraulic characteristics of cavernous weathering rocks forming tafoni and honeycombs. MSc. Theses, Charles University, Faculty of Science, Prague (in Czech).

Sunamura T. (1996) A physical model for the rate of coastal tafoni development. J. Geol. 104 (6), 741–748.

Tan S.A. (1989) A simple automatic falling head permeameter. Soils and Foundations, 29(1), 161-164.

Tetens O. (1930) Über einige meteorologische Begriffe. Zeitschrift für Geophysik, 6, 207–309.

Van Genuchten M.T. (1980) A closed-form equation for predicting the hydraulic conductivity of unsaturated soils. Soil Sci. Soc. Am. J. 44, 892–898.

Viles H.A. and Goudie A.S. (2004) Biofilms and case hardening on sandstones from Al-Quwayra, Jordan. Earth Surface Processes and Landforms 29, 1473–1485.

Viles H.A., Goudie A.S., Grab S., Lalley J. (2011) The use of the Schmidt Hammer and Equotip for rock hardness assessment in geomorphology and heritage science: a comparative analysis. Earth surface processes and landforms 36, 320–333.

Washburn E.W. (1921) Dynamics of capillary flow. Phys. Rev. 17, 273–283.

Weiss T., Slavík M. and Bruthans J. (2018) Use of sodium fluorescein dye to visualize the vaporization plane within porous media. Journal of Hydrology, 565, 331–340.

Weiss T., Mareš J., Slavík M. and Bruthans J. (2020) A microdestructive method using dye-coated-probe to visualize capillary, diffusion and evaporation zones in porous materials. Science of The Total Environment 704, 135339.

Weiss T., Kalianková K., Slavík M., Mareš J., Maříková-Kubková J., Válek J. (2022) Methods of moisture measurement in historical masonry with examples of use on archaeological sites under the third courtyard of Prague Castle (in Czech). Journal of Historical Heritage Preservation, 82(1), 88-96.

Weiss T. and Sass O. (2022) The challenge of measuring rock moisture–a laboratory experiment using eight types of sensors. Geomorphology 416, 108430.

Yu S. and Oguchi C.T. (2010) Role of pore size distribution in salt uptake, damage, and predicting salt susceptibility of eight types of Japanese building stones. Engineering Geology 115(3–4), 226–236.